Research paper

Influence of selected technological parameters on dynamic replacement column formation – results of laboratory model tests

Sławomir Kwiecień[1], Siergey Ihnatov[2], Magdalena Kowalska[3]

Abstract: The paper presents results of the research on the influence of selected technological parameters on dynamic replacement columns formation. The analysis concerned: the depth of the initial crater H_{cr}, the volume of its filling V_{cr}, and the grain size of the backf used. It was carried out on a testing stand that allowed the observation and documentation of the particle driving process. The soft soil layer was simulated with a hydrogel, while the bearing layer was made of medium sand. The columns were formed in the initial craters, with a depth of 0.4, 0.6 or 0.8 of the thickness of the soft layer, and backfilled up to 50, 75 or 100% of the volume. The investigation of the optimal crater and backfill volume was carried out using medium gravel (2–16 mm). The influence of the grain size of the backfill material was studied at the optimal H_{cr} and V_{cr} – medium sand (0.063–2 mm) and medium gravel (2–32 mm) were used at this stage. The displacements of backfill material grains and the shapes of the columns were analysed using GOM and Cad software. The optimal solution was to construct the columns in the shallow crater ($H_{cr}/H_s = 0.4$) and to backfill it with gravel 2–16 mm up to 50% of the volume – under these conditions, end-bearing columns were formed with the diameter increasing with depth. In order to improve the shape of the column, in the final phase of the DR process, V_{cr} shall be increased up to 100%.

Keywords: dynamic replacement, ground improvement, soft soil, stone columns

[1]DSc., PhD., Eng., Silesian University of Technology, Faculty of Civil Engineering, ul. Akademicka 5, 44-100 Gliwice, Poland, e-mail: slawomir.kwiecien@polsl.pl, ORCID: 0000-0001-6401-2471
[2]PhD., Eng., KG Construction Sp. z o.o., ul. Gornicza 33, 43-173 Laziska Gorne, Poland, e-mail: siarhej.ign@gmail.com, ORCID: 0000-0002-5747-291X
[3]PhD., Eng., Silesian University of Technology, Faculty of Civil Engineering, ul. Akademicka 5, 44-100 Gliwice, Poland, e-mail: magdalena.kowalska@polsl.pl, ORCID: 0000-0001-7549-2722

1. Introduction

Dynamic replacement method (DR) is a popular deep ground improvement technique that has been invented by Louis Ménard in 1975 [1]. It consists in driving a coarse-grained material into a weak soil by means of repeated drops of a heavy pounder. The aim is to create a stronger column in the ground capable of transferring the load directly to the underlying bearing layer and partially to the surrounding weak ground. In addition, drainage conditions are usually improved. A successful procedure should result in an end-bearing column with its base resting on the stronger soil layer. During the DR process, the shape and dimensions (length and diameter) of the column cannot be directly controlled. As reported in the literature [2, 3], it is possible to create an end-bearing column in the soft layers as thick as 8–9 m. However, the practical experience of the authors gained on several construction sites in Poland (30 columns examined *in situ*) shows that despite the thickness of the soft layers not exceeding 5 m, the DR columns do not reach the bearing layer [4, 5] (floating columns). The reason for this is most likely to lie in the technological parameters used by the contractors, such as the height of the pounder drop, the depth of the crater, the volume and/or the grading of the backfill material. As a full-scale *in situ* study of this problem is very costly and time-consuming and does not provide any insight into the mechanisms responsible for the displacement of the backfill material, the authors decided to carry out a medium-scale laboratory study to identify the main factors responsible. A testing stand in the form of a rectangular box with an acrylic glass front was prepared [6]. The very soft soil layer was modelled with a semi-transparent acrylic polymer to allow observation and documentation of the entire DR process using a high-speed camera. In the current study we focused on the following technological parameters: crater depth, backfill grading and volume, and impact energy. The research presented here is a continuation of the previous investigations [6, 7]. The former [6] concentrated on the influence of the thickness of the soft soil on the displacement paths of the backfill aggregate during the driving process. The latter [7] was a preliminary study, limited to single columns and only one type of backfill material.

2. Importance of dr column shapes in the load transfer

The lengths and shapes of the DR columns are highly variable. In the literature, see Table 1, four different shapes are typically distinguished in field tests: cylindrical, truncated cone, inverted truncated cone and barrel (symmetrical or asymmetrical) [4, 5, 8–14, 17]. The shape of the columns depends on the technological parameters used and on the ground conditions (thickness and plasticity of the soft layer). In the case of end-bearing columns, it is directly influenced by the ratio between the thickness of the soft layer (H_s) and the height of the pounder (H_p), as shown by Kwiecień *et al.* [6] and Kwiecień and Kowalska [17]. If H_s/H_p does not exceed 2.44–2.93 [5, 15], it is usually possible to construct end-bearing columns. The construction of floating columns in ground conditions with a smaller H_s/H_p ratio, e.g. 1.89–2.22 [5, 14], means that the technological parameters have been incorrectly assumed.

Table 1. DR column shapes in literature

Author(s)	Ground conditions	D_c/D_p [–]	M_p/H_d [Mg/m]	H_s/H_p [–]	Type/Shapes of columns
Lo *et al.* [8]	0–5.8 m: peaty clay from 5.8 m: old alluvium	n.d.	15/15	n.d.	floating/ inverted truncated cone
Gunaratne *et al.* [9]	0–1.2 m: working platform 1.2–3.0 m: organic soil from 3.0 m: silty sand	2.46	4/12	2.14	end-bearing/ cylindrical
Kumar [10]	0–0.6 m: fill 0.6–1.5 m: medium stiff sandy silt 1.5–3.0 m: medium stiff silty clay 3.0–12.5 m: loose fine and medium sand	1.0–1.25	19/21	n.d.	end-bearing/n.d.
Chua *et al.* [11]	0–2 m: loose sand (fill) 2–3 m: soft clay 3–10 m: medium dense to dense sand	n.d.	24–26/ 10–20	n.d.	end-bearing/ inverted truncated cone
Kwiecień and Sękowski [12]	various ground conditions (11 columns)	1.5–2.7	10.5–12.0/ 15–25	0.5–1.9	end-bearing/cylindrical, barrel
Varaksin and Hamidi [13]	0–1.5 m: disturbed clay from 1.5 m: very stiff clay	1.41	38.5/5	2.22–2.89	floating/ cylindrical, barrel
Kwiecień and Sękowski [14]	various ground conditions (32 columns)	1.23–4.1	9–12/15–25	0.5–2.93	end-bearing/cylindrical, inverted truncated cone, barrel
Sękowski *et al.* [15]	0–1.5 m: working platform (semi-dense medium sand) 1.5–3.2 m: soft organic mud 3.2–5.0 m: semi-dense medium sand	1.7–2.4	11 /10	1.94	end-bearing/ inverted truncated cone
Danilewicz [15]	0–1.9 m: working platform (semi-dense medium sand) 1.9–5.7 m: organic soil 5.7–8.73 m: medium dense fine sand	n.d.	n.d.	2.22–2.89	floating/ cylindrical, barrel
Kwiecień [4,5]	various ground conditions (65 columns)	n.d.	9–24/15–25	0.5–2.44	end-bearing columns/ cylindrical, truncated cone, barrel, asymmetrical barrel
				1.89–4.17	floating columns/ cylindrical, barrel, inverted truncated cone
Kwiecień and Kowalska [17]	various ground conditions (18 columns)	1.4–2.8	9–11.5/15	0.85–2.11	end-bearing columns/ cylindrical, truncated cone, barrel, asymmetric barrel

D_c – diameter of the column, D_p – diameter of the pounder, H_p – height of the pounder, H_s – thickness of the soft soil, M_p – mass of the pounder, H_d – height of the pounder drop, n.d. – no data

Trial plate load tests and numerical analyses using the finite element method (FEM) carried out by Kwiecień [4,5], have shown that the shape of the DR column and the way it is supported (end-bearing or floating) have a tremendous effect on its load-bearing capacity and stiffness. They are highest for the end-bearing columns with flat bases, and get enhanced in the cases where the column diameter increases with depth, as illustrated in Fig. 1a. On the other hand, the floating columns with diameters decreasing with depth, as shown in Fig. 1b, have the lowest bearing capacity and stiffness. Therefore, in practice, it seams reasonable to try to make the end-bearing columns in the shape of a truncated cone. This will only be possible if the technological parameters applied during construction, such as the depth of the initial crater, the volume of the backfill, the impact energy and the grading of the backfill material, are optimal.
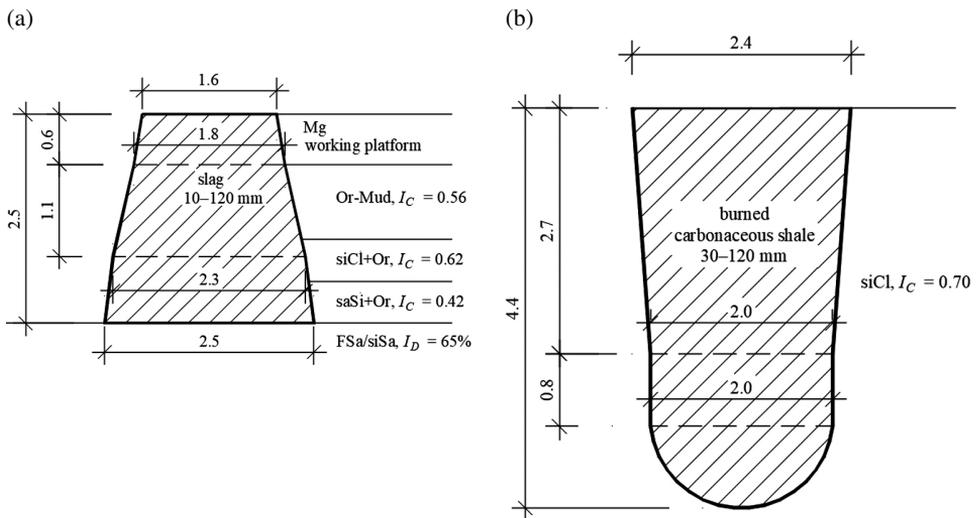

Fig. 1. Exemplary shapes and dimensions of DR columns exhibiting very high (a) and very low (b) load-bearing capacity and stiffness [5] (dimensions in meters; I_C – consistency index)

3. Testing stand and materials used

The experiments were carried out in a rectangular test box with the external dimensions of 1.5 m (width) $\times$ 1.0 m (height) $\times$ 0.15 m (thickness), showed in Fig. 2. An acrylic glass pane was used as the front wall to allow observation of the dynamic replacement process.

Two layers of soil were modelled: a bearing layer at the bottom and a soft layer at the top. The latter, 50 cm thick (H_s = 0.5 m), consisted of a semi-transparent hydrogel – prepared by mixing a cross-linked hydrophilic water-soluble acrylic polymer (p) and room-temperature potable water (w) in the ratio p/w = 1:15 (by weight). The consistency of the hydrogel mixture was very soft, as determined by cone penetration tests accordingly to ISO 17892-12 [18]. Its average density was equal to 1010 kg/m^3. The bottom layer was made of medium sand MSa (0.063–2 mm), which was carefully compacted in three or four layers of 10 cm each, using a tamper, to obtain the 0.4 m (*Series 1*) or 0.3 m (*Series 2* and *Series 3*) thick bearing

layer with a density index $I_D = 0.44$. The thickness of the MSa layer was reduced after the first series of the experiments to provide more space above the very soft hydrogel layer, which tended to be pushed out of the box during some DR processes.

Three different materials were used to form the DR columns: medium gravel MGr_1 (2–16 mm), medium gravel MGr_2 (2–32 mm) or medium sand MSa (0.063–2 mm) – the same as in the bearing layer.

The physical and mechanical properties of the sand and gravels used are presented in Table 2 and Table 3. They include the mean particle diameter d_{50}, the coefficient of uniformity C_U and the coefficient of curvature C_C, the minimum and maximum dry densities ($\rho_{d.min}$, $\rho_{d.max}$), the specific density ρ_s, the peak angle of internal friction φ, as well as the primary and secondary constrained compression moduli, M_0 and M. For details of the laboratory procedures used to determine these parameters, the reader is referred to [6].
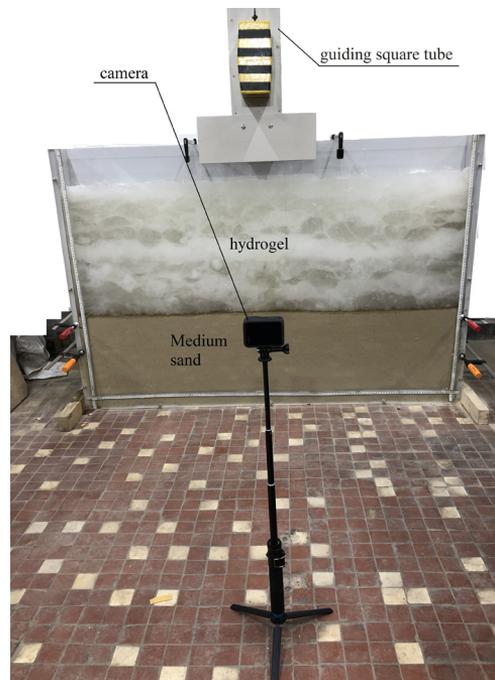

Fig. 2. The testing stand prepared for execution of a DR column [6]

Table 2. Physical properties of the soils used

#	Type of soil	d_{50} [mm]	C_U [–]	C_C [–]	ρ_s [kg/m³]	ρ_{dmin} [kg/m³]	ρ_{dmax} [kg/m³]
1.	MSa (0.063–2 mm)	0.30	3.33	0.92	2683	1592	1936
2.	MGr_1 (2–16 mm)	9.70	3.43	1.59	2658	1500	1830
3.	MGr_2 (2–32 mm)	12.0	3.57	1.53	2658	1620	1850

Table 3. Mechanical properties of the soils used

#	Type of soil	ρ_d [kg/m^3]	φ [°]	M_0 [MPa]*,**	M [MPa]**
1.	MSa (0.063–2 mm)	1590	29.9	4.1–38.0	14.5–93.5
2.		1800	33.6	8.3–74.9	38.0–108.5
3.	MGr_1 (2–16 mm)	1530	36.1	6.2–44.8	93.3–124.1
4.		1820	42.5	19.6–102.9	100.4–192.9
5.	MGr_2 (2–32 mm)	1640	33.5	3.2–39.6	68.1–119.7
6.		1840	35.3	13.5–140.8	149.3–253.5

*For comparison with M – the M_0 values are given for the stress range 25–800 kPa
**The former value represents the range 25–50 kPa, the latter: 400–800 kPa

To estimate the mechanical properties of the hydrogel layer, a plate loading test was carried out on the testing stand. A wooden plate measuring $123 \times 124 \times 18$ mm was placed on the top surface and loaded up to 0.285 kPa. The measured displacement of the plate was then used in a 2D FEM back-analysis, in which the material was described using an elastic-perfectly plastic Coulomb–Mohr constitutive model. The following results were obtained: Young modulus $E = 7$ kPa, angle of internal friction $\varphi = 0.4°$, cohesion $tc = 0.075$ kPa.

In order to drive the backfill material into the soft layer, a barrel-like pounder was dropped from a specified height through a square guiding tube as shown in Fig. 2. The mass of the pounder was 11 kg, and its heigh H_p and base width D_{bp} were 200 mm and 90 mm, respectively. It is worth noting that the ratio of the grading of the backfill material to the width of the pounder base was equal to 0.00–0.02/0.02–0.18/0.02–0.36 for MSa/MGr_1/MGr_2.

The displacement paths of the backfill grains were recorded with a high-speed camera (100 frames per second) and analysed using GOM [19] and Autocad software. Photographs were also taken at each stage of the tests. A detailed description of the test box, equipment and software used can be found in [6].

4. Research program

In the previous research carried out on the same testing stand [6], it was shown that at $H_s/H_p = 2.5$, the DR columns formed of MGr_1 in the 0.5 m thick hydrogel layer exhibited semi-circular bases and reached the MSa bearing layer only pointwise. Therefore, they shall be treated as floating columns, being a non-optimal solution. It was decided to continue the study with the same soft layer thickness in order to show the influence of diffrent technological parameters on the DR process and the resulting shape and manner of the column support on the bearing layer. The following parameters were varied: the depth of the initial crater H_{cr}, the volume of its backfill V_{cr}, the impact energy E_d and the backfill material grade d_m.

The following DR process was applied: (1) a square metal tube 11.5×11.5 cm, closed at the bottom with a plate, was gently pushed into the hydrogel layer to the planned depth of the initial crater H_{cr}; (2) the closing plate was removed; (3) the inside of the pipe was filled with the planned volume of the backfill material V_{cr}, followed by removal of the pipe with the use of slight vibration; (4) due to the hydrogel being sucked up during the removal of the closing plate, more backfill material was added and pushed by means of the closing plate to adjust the depth of the crater and V_{cr}; (5) the guiding tube was placed on the edge of the box; (6) the pounder was dropped onto the backfill surface from the height that varied between 0.2 and 1.4 m – it was adjusted so that the displacement of the top surface of the column backfill ΔH was equal to 0.75–$1.50 H_p$; (7) the created crater was filled with the backfill material up to the planned V_{cr}, unless ΔH was less than $0.75 H_p$ – then the backfill material was not added. Steps (6) and (7) were repeated until the observed penetration of the column base became negligible and further pounder drops resulted only in widening of the column top surface. After each column was completed and documented, the backfill material was removed, the void was replaced with an appropriate amount of hydrogel and the stand was prepared ready for the next test.

Three versions of the DR columns were formed, differing in the depth of the initial crater: (A) $H_{cr} = 0.2$ m ($H_{cr}/H_s = 0.4$), (B) $H_{cr} = 0.3$ m ($H_{cr}/H_s = 0.6$) and (C) $H_{cr} = 0.4$ m ($H_{cr}/H_s = 0.8$). The crater was backfilled up to $V_{cr} = 50\%$ (columns A), 75% (columns B and C) or 100% (columns A, B, C) volume. In the columns B and C, the minimum V_{cr} tested was 75% because the slopes of the crater showed instability at 50%. The cases analysed are further indicated in the text as A_50, B_75, C_75, A_100, B_100, C_100.

The optimal H_{cr} and V_{cr} were determined using the MGr_1 backfill material, defined as the one at which the end-bearing instead of floating columns were obtained. Keeping these technological parameters constant, two more column versions were prepared, this time using the MGr_2 and MSa backfill materials to show the influence of the grading.

A summary of the all the columns tested is given in Table 4. Each test was repeated twice (in *Series 1* the MSa bearing layer was 40 cm thick, while in *Series 2* and *Series 3* – it was 30 cm thick), so a total of 24 columns were prepared and analysed.

Table 4. Summary of the research program

#	Type of column	Backfill material	H_{cr} [m]	H_{cr}/H_s [–]	V_{cr} [%]
1.	A_50 (MGr_1)		0.2	0.4	50
2.	A_100 (MGr_1)				100
3.	B_75 (MGr_1)	MGr_1(2–16 mm)	0.3	0.6	75
4.	B_100 (MGr_1)				100
5.	C_75 (MGr_1)		0.4	0.8	75
6.	C_100 (MGr_1)				100
7.	A_50 (MGr_2)	MGr_2(2–32 mm)	0.2	0.4	50
8.	A_50 (MSa)	MSa (0.063–2 mm)	0.2	0.4	50

5. Results

The photographic documentation of the representative columns made of MGr_1 backfill, together with the vectors of the resultant displacements, are presented in Fig. 3 and Fig. 4, after [7]. The column shapes are shown after a selected number of pounder drops, allowing their evolution during the DR process to be observed.

As can be seen in Fig. 3a, when the column is formed in the relatively shallow, completely backfilled crater (A_100 type), the largest vertical displacements of the grains are observed along the column axis. With successive drops of the pounder, the resulting semi-cylindrical base of the column gradually moves downwards (Fig. 3d) and increases in diameter, as seen in Fig. 3g. In the final DR phase, the largest grain displacements are observed in the upper part of the column (Fig. 3g). The final shape of the column is pear-like, with only a point support on the end-bearing MSa layer, as shown in Fig. 3j. The result is in full agreement with the previous study presented in [6].

As the depth of the initial crater is increased (column B_100), the axis of the column starts to deviate from the vertical, as shown in Fig. 3b, e. As the number of pounder drops increases and inclination of the bottom part of the column reaches approximately 70°, the column breaks and the backfill material starts to accumulate on the other side – Fig. 3e, h. The base of the column ends up irregularly shaped and does not reach the bearing layer. The diameter of the column above is relatively constant, but begins to decrease when approaching the surface – Fig. 3k.

The behaviour of column C_100 with the deepest initial crater and complete backfill is even more complicated. Initially, the displacement of the grains is mostly vertical (Fig. 3c), but as the number of pounder drops gets higher, the diameter of the column increases at the very top of the column (the grains move sideways), while at the bottom the axis of the column deviates from verticality (Fig. 3f) – similar to the case B_100. As inclination of the bottom part of the column increases, part of the backfill starts to move sideways – Fig. 3j. Finally, the bearing layer is reached only at one point, as can be seen in Fig. 3i, l. The final shape of the column is very irregular and asymmetrical (Fig. 3l).

In column A_50, where the initial crater was shallow and only partially filled, the backfill material also initially moved vertically towards the end-bearing layer (Fig. 4a, d), but later the grains at the bottom started to displace sideways (Fig. 4g). The result was a flat-bottomed, pear-shaped column, as shown in Fig. 4j. In order to increase the diameter of the A_50 column in its upper part, it was decided to fill the crater completely ($V_r = 100\%$) in *Series 3*, after the base of the column had been formed at the 22nd drop of the pounder – the procedure was successful, as can be seen in Fig. 5.

The dominant vertical downward movement of the backfill grains at the beginning of the DR process (1st or 2nd drop of the pounder) was also observed in the columns B_75 and C_75 (Fig. 4b, c). In the column B_75, before the backfill reached the bearing layer, the axis of the column started to deviate from the vertical (Fig. 4e) reaching an angle of up to 70° (Fig. 4h, k). The backfill material begun to move sideways resulting in a discontinuity in the column shaft. The final shape of the column resembles a slender pear with only a point support on the bearing layer, as shown in Fig. 4k. The behaviour of the column C_75 was similar (Fig. 4c, f, i, j), although the discontinuity mentioned above was observed at an earlier stage of the process – see Fig. 4f.
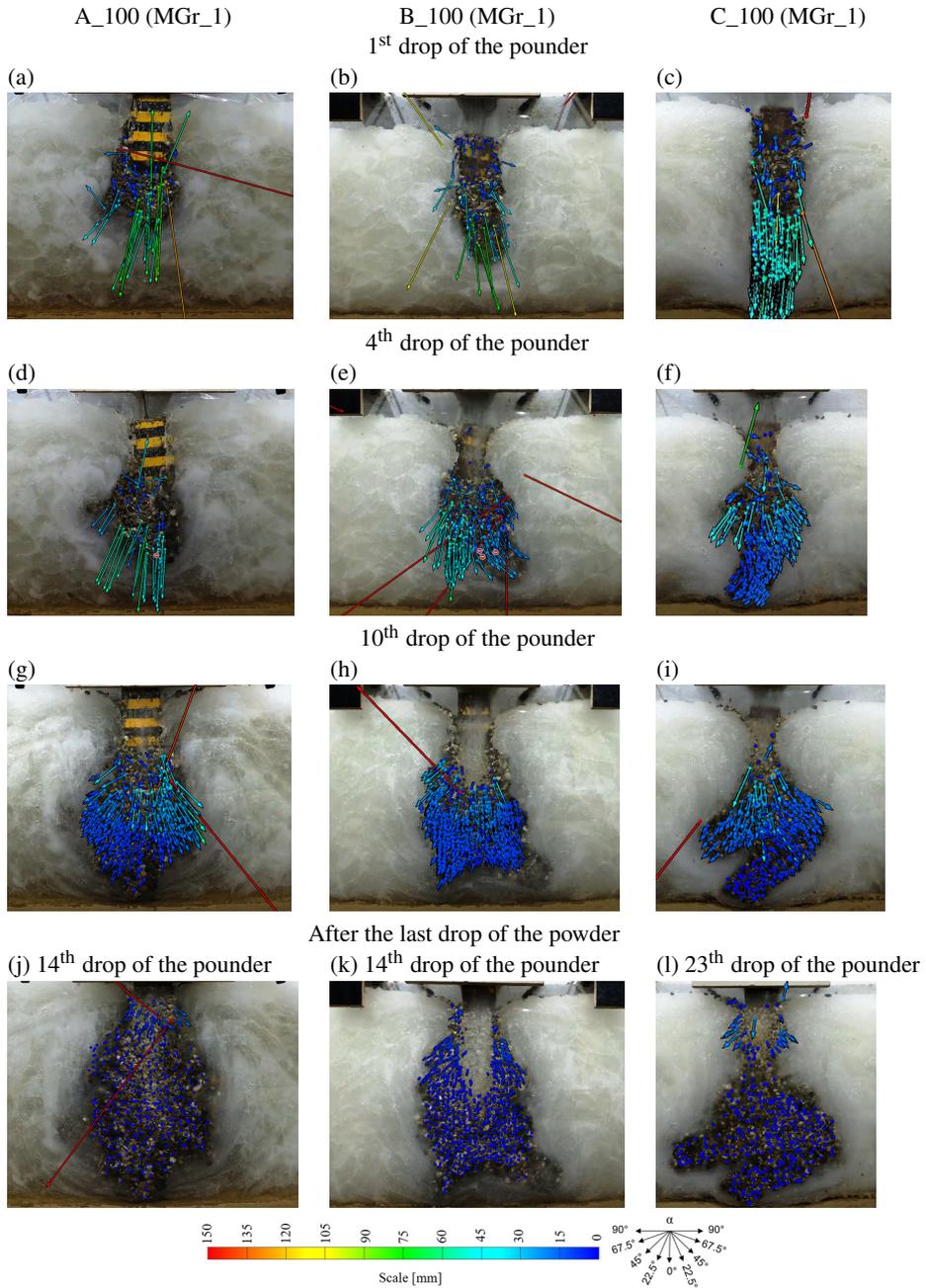
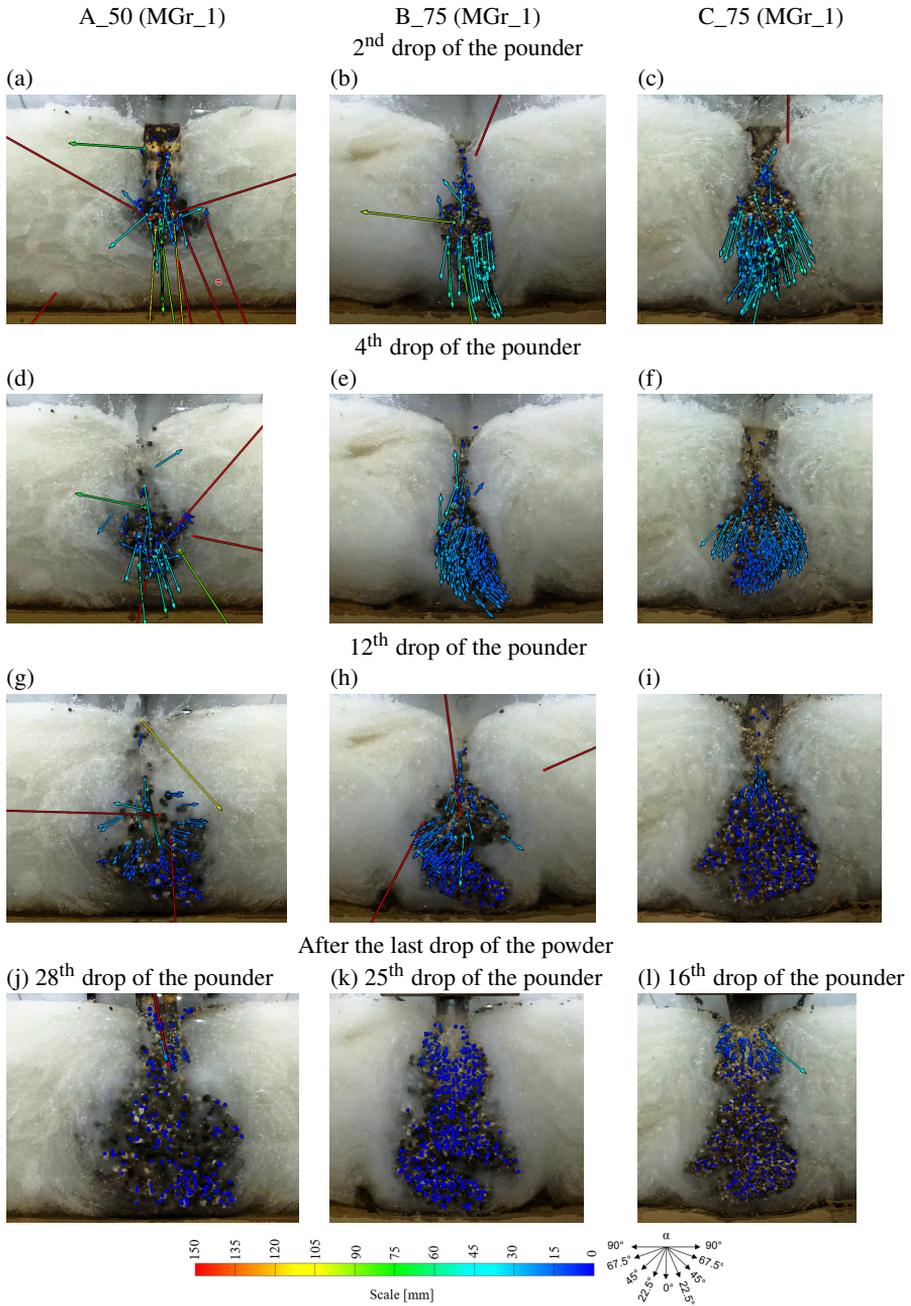Fig. 3. The vectors of the resultant displacements – columns A_100, B_100 and C_100, complete backfill with MGr_1 [7]

Fig. 4. The vectors of the resultant displacements – columns A_50, B_75 and C_75, backfill with MGr_1 [7]

(a)   (b)   (c)

Fig. 5. Final shapes of the A_50 (MGr_1) columns: (a) *Series 1* [7] , (b) *Series 2*, (c) *Series 3*

Of all the columns made of MGr_1 backfill material, only the A_50 types can be classified as end-bearing – with the base of the column clearly supported on the bearing layer. The diameter of these columns increased with depth – therefore high load-bearing capacity and stiffness can be expected.

The total impact energy E_t, calculated as the sum of the mass of the pounder multiplied by gravity and the height of the fall for all drops, divided by the area of the pounder's base, is plotted against the number of drops of the pounder N in Fig. 6. It can be seen that the smallest increase in E_t occurred in the columns that were formed with partial backfilling of the crater. Furthermore, as shown in Fig. 7, the total energy required to cause the bottom of the backfill to reach the MSa layer and achieve a stable length of the column ($\geq H_s$) was approximately 80 kNm/m^2 (at $N = 15$) in the case of A_50, whereas for A_100 and B_75 this was achieved with a much higher energy of 147 kNm/m^2 and 156 kNm/m^2 (both at $N = 13$), respectively, cf. Fig. 7. Interestingly, the amount of gravel required at this stage of the process in column A_50 was much less than in the other columns, cf. Fig. 8.
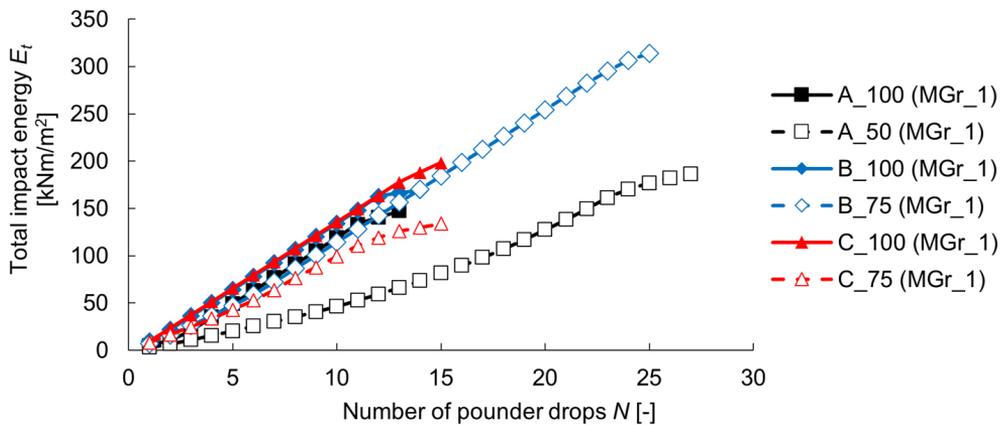

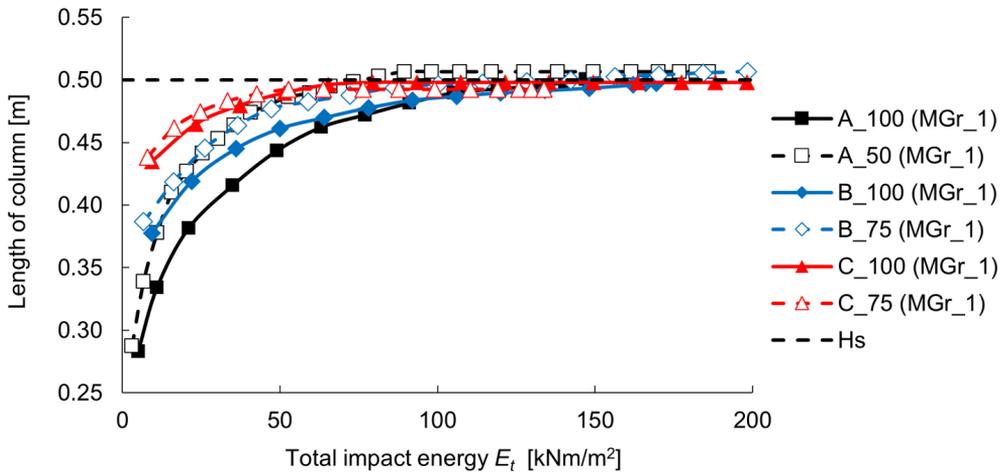Fig. 6. Total impact energy used in column formation (mean value)

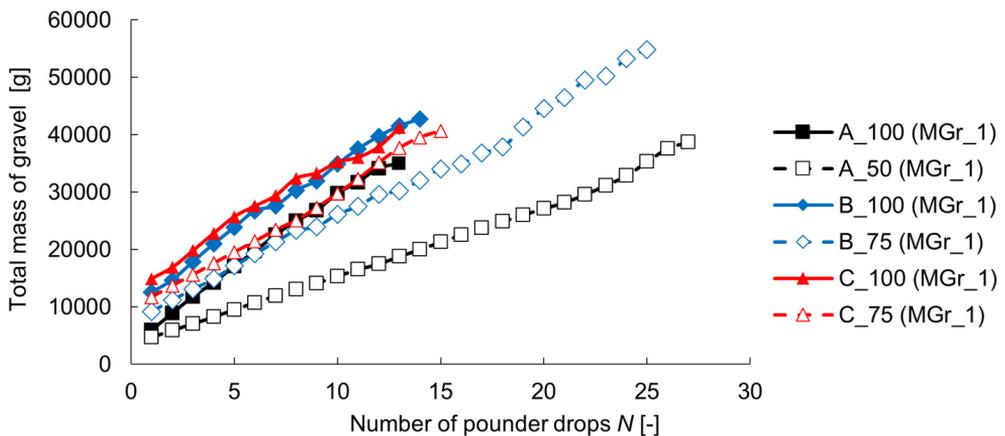Fig. 7. Evolution of the length of the columns during formation (mean value)

Fig. 8. Total mass of gravel used in column formation (mean value)

Considering the fact that the A_50 (MGr_1) column was end-bearing and potentially also optimal in terms of cost of execution, it was decided to further study the influence of the grading of the backfill material on the columns formed in the initial crater 0.2 m deep and with partial backfilling of the crater $V_{cr} = 50\%$. At this stage of the investigation, they were carried out using MGr_2 (2–32 mm) and MSa (0.063–2 mm) backfill materials. The MSa grading was too fine to use the GOM software for the grain displacement analysis, therefore only the shape and dimensions of these columns were analysed using photographic documentation and Autocad software. The results are presented in Fig. 9.
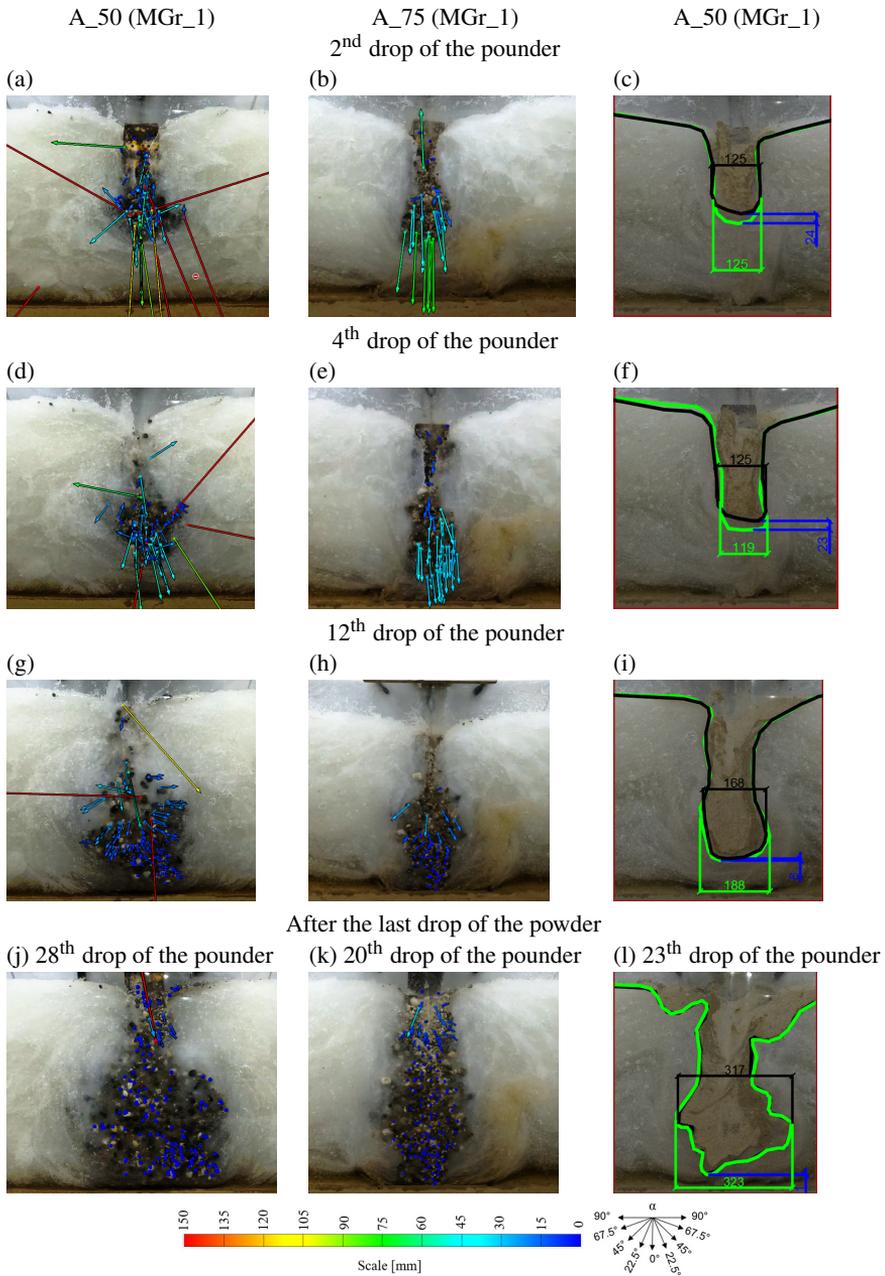
Fig. 9. Columns A_50: the vectors of the resultant displacments, partial backfill with MGr_1 (a) and MGr_2 (b); shapes and dimensions, partial backfill with MSa (c)

It was observed that the MGr_2 grains were wedged between the box walls, causing some random displacements and non-uniformity of the behaviour in *Series 1–3*. The resulting A_50 columns had diameters and areas of contact with the bearing layer much smaller than in the cases where MGr_1 was used, as can be seen in Fig. 9b, e, h, k. The behaviour of the MSa backfill was more similar to the A_50 (MGr_1) case: initially, it moved vertically towards the end-bearing layer (Fig. 9c, f), but the diameter of the column started to increase before the material reached the bearing layer (Fig. 9i, l). Eventually, the base of the column was not flat and had only point contact with the lower layer; the column was not symmetrical along its axis, cf. Fig. 9l. It was noticed that the pounder was not effectively pushing the whole mass of the MSa backfill material, see Fig. 9l, but was penetrating it, causing increase in the diameter of the column at the surface of the hydrogel layer.

The increase of the average length of the columns was slower or only slightly slower when MSa or MGr_2 backfill material was used, compared to the MGr_1, as can be seen in Fig. 10. The total impact energy that was applied depending on the actual pounder drive, increased with the maximum grading of the backfill material – the coarser the material used, the greater it was, cf. Fig. 11. Comparing the mass of the material used for the same number of pounder drops, see Fig. 12, slightly more MGr_2 was required than MGr_1 or MSa, which is directly related to the higer impact energy.
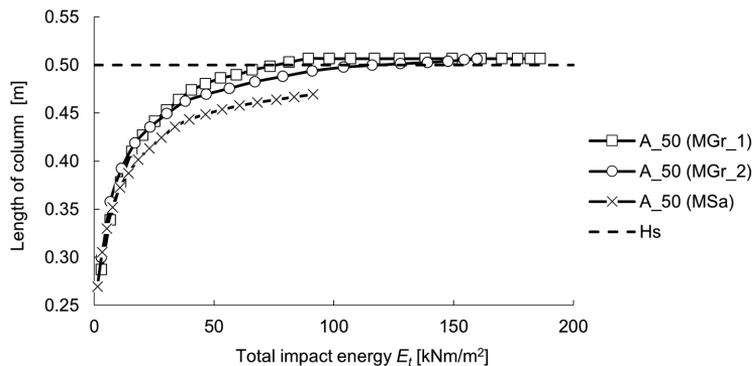

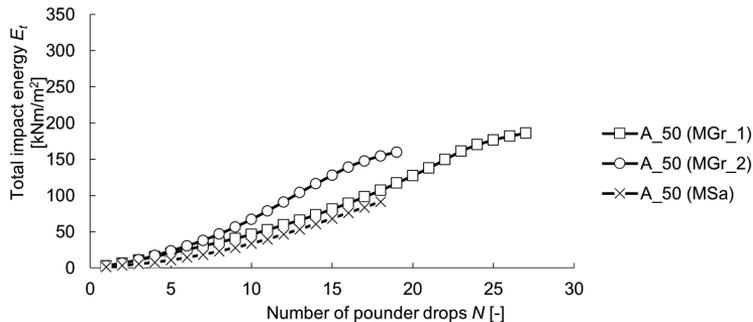Fig. 10. Evolution of the length of the columns during formation (mean value) – columns A_50

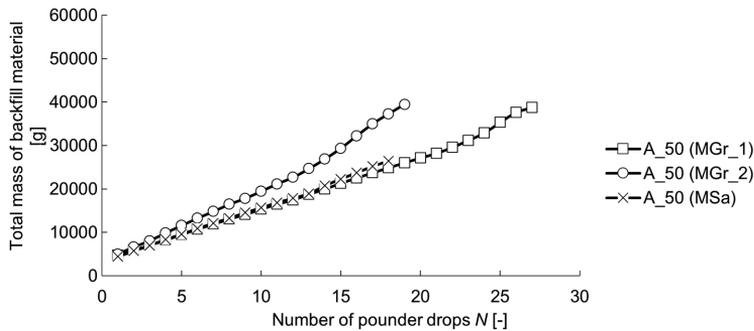Fig. 11. Total impact energy used in column formation (mean value)

Fig. 12. Total mass of backfill material used in column formation (mean value)

6. Discussion and conclusions

Based on the results presented above, it can be concluded that all the technological parameters studied: (i) the depth of the initial crater, (ii) the volume of the backfill added before the pounder is dropped, and (iii) the grading of the backfill material, have a strong influence on the final volume and shape of the DR column, as well as on the impact energy, necessary to obtain a reliable ground improvement.

The deeper craters ($H_{cr}/H_s = 0.6$ and 0.8) completely filled with the backfill material, represented by the columns B_100 (MGr_1) and C_100 (MGr_1), require the highest amount of impact energy at the beginning of the DR process, as shown in Fig. 6. This is due to the fact that the vertical stress increase caused by the drop of a pounder onto the top surface of the backfill column decreases with depth and is therefore smaller under a taller backfill column than under a shorter one – leaving less energy to push the backfill mass into the soft layer. In addition, under a deeper crater, the distance between the bottom of the backfill and the upper boundary of the bearing layer is smaller, causing the backfill grains to move not only downwards but also sideways, as demonstrated in [6] – this process consumes some of the energy applied. The total impact energy, caused mainly by larger pounder drive, is required when the crater is shallower (A_100) and continues to decrease as the volume of backfill used decreases – the lowest values were recorded in columns A_50 (MGr_1) and A_50 (MSa) – see Fig. 6 and Fig. 11. The smaller V_{cr} in the columns A_50 and B_75, made of the MGr_1 material, required a higher number of the pounder drops, as can be seen in Fig. 8, although the drops were made from lower heights. As the depth of the initial crater increases, a greater mass of the backfill material is required, as can be seen in Fig. 8. This is due to the fact that more material is required to counteract the deviation of the column axis from verticality and sideways displacement of the material, causing an excessive increase in the diameter of the column far from its base.

The optimal column in terms of load-bearing capacity is the one whose base is flat and strongly supported on the bearing layer, and whose diameter gradually increases with depth (truncated cone shape). This condition was met by column A_50 (MGr_1) with $H_{cr}/H_s = 0.4$ and $V_{cr} = 50\%$, confirming the results of the preliminary study [7] carried out in only one

series. The diameter of column A_100 (MGr_1) with $V_{cr} = 100\%$ also increased with depth, but at too early stage, leading to increased resistance to penetration and ultimately unsatisfactory support on the bearing layer.

Columns B and C with the deeper initial craters, both partially or completely backfilled, were characterised by greater slenderness than columns A and were therefore more likely to be bent and sheared during compaction. This resulted in poor contact with the bearing layer and discontinuities in the column shaft (the only exception being column B_75). It should be noted that under field conditions, the crane will repeatedly set the pounder aside and lift it over the planned improvement point as the crater is filled – during these operations there is a high probability that the pounder will fall eccentrically, increasing the risk of the column shaft deviating from verticality.

It is worth noting that the column with the optimal shape (A_50) was formed using the slowest increasing total impact energy (the pounder fell from the smallest heights). In practice, this may mean that it is possible to produce such a column with relatively small equipment, provided that the crater depth and backfill volume are adequate.

The ratio of the observed vertical displacement of the column base on its axis S_c to the actual average drive of the pounder S_p versus the number of pounder drops for the optimal column A_50 (MGr) is shown in Fig. 13. In practice, this graph can be used as a guide for the design of end-bearing DR columns, where the following conditions are met: $H_s/H_p = 2.5$, $H_{cr} = H_p$, $V_{cr} = 50\%$ up to the 22nd drop, and $V_{cr} = 100\%$ for later final filling. The first 11 drops are responsible for forming the shaft of the column with the base reaching the bearing layer, while the next 11 drops make the base flat. The purpose of the later drops is to increase the diameter of the column head.
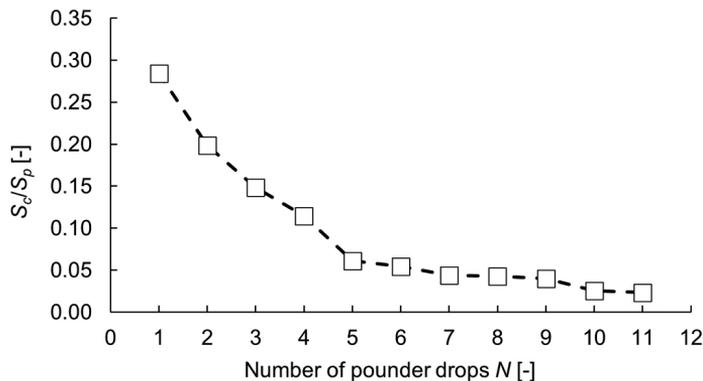

Fig. 13. The influence of the number of pounder drops on the S_c/S_p ratio for column A_50 (MGr_1)

The described study did not consider the influence of the consistency of the soft layer or the shape of the pounder used on the column forming technique – this is planned in the further stage of the laboratory and/or field research.

The authors are aware of the qualitative nature of the research, which is influenced, among other things, by (i) the effect of the scale or (ii) the limitation for the aggregate to move only in two dimensions, causing an excessive increase of the column diameter in the observed plane.

Nevertheless, the results presented provide a preliminary basis for future research to be carried out at full scale, in soils of low strength and stiffness (e.g. peat), and for the development of guidelines for the optimal dynamic replacement technique.

Acknowledgements

References

[1] B. Hamidi, "Distinguished ground improvement projects by dynamic compaction or dynamic replacement", PhD thesis, Curtin University, Australia, 2014.

[2] J. Guo, R. Wang, Z. Yang, and C. Zhu, "Mucky clay treatment by dynamic compacted gravel column method", *Rock and Soil Mechanics*, vol. 14, no. 2, pp. 61–74, 1993.

[3] J. Chu, S. Varaksin, U. Klotz, and P. Mengé, "Construction processes. State of the art report", in *Proceedings of the 17th International Conference on Soil Mechanics and Geotechnical Engineering, Alexandria*. IOS Press, 2009, pp. 3006–3135.

[4] S. Kwiecień, "Influence of load plates diameters, shapes of columns and columns spacing on results of load plate tests of columns formed by dynamic replacement", *Sensors*, vol. 21, no. 14, art. no. 4868, 2021, doi: 10.3390/s21144868.

[5] S. Kwiecień, *The deformability of dynamic replacement columns based on in-situ load tests*. Gliwice, Poland: SUT Press, 2019 (in Polish).

[6] S. Kwiecień, S. Ihnatov, and M. Kowalska, "Influence of soft layer thickness on the aggregate displacement in the backfill material of dynamic replacement columns – results of laboratory model tests", *Archives of Civil Engineering*, vol. 69, no. 3, pp. 253–268, 2023, doi: 10.24425/ace.2023.146079.

[7] S. Kwiecień and S. Ihnatov, " Influence of the dynamic replacement technology on the shape of columns in laboratory conditions", *Materiały Budowlane*, no. 10, pp. 32–38, 2023, doi: 10.15199/33.2023.10.07 (in Polish).

[8] K.W. Lo, P.L. Ooi, and S.L. Lee, "Unified approach to ground improvement by heavy tamping", *Journal of Geotechnical Engineering,* vol. 116, no. 3, pp. 514–527, 1990, doi: 10.1061/(ASCE)0733-9410(1990)116:3(514).

[9] M. Gunaratne, G. Mullins, P. Stinnette, and S. Thilakasiri, *Stabilization of Florida organic material by dynamic replacement. Final report of State Project no. 99700-3541-119*. Department of Civil and Environmental Engineering, Tampa, Florida, 1997.

[10] S. Kumar, "Reducing liquefaction potential using dynamic compaction and construction of stone columns", *Geotechnical and Geological Engineering*, vol. 19, pp. 169–182, 2001, doi: 10.1023/A:1016672106067.

[11] Ch. Chua, M. Lai, G. Hoffmann, and B. Hawkins, "Ground improvement using dynamic replacement for NCIG Cet3 Coal Stockyard", *Australian Geomechanic*, vol. 43, no. 3, pp. 63–74, 2008.

[12] S. Kwiecień and J. Sękowski, "Research on the shape of stone columns formed in the ground with the use of dynamic replacement method", *Architecture Civil Engineering Environment*, no. 2, pp. 65–72, 2008.

[13] S. Varaksin and B. Hamidi, "Ground improvement case histories and advances in practice", in *Transport infrastructure development and natural hazards mitigation: Proceedings of the International Conference on Ground Improvement and Ground Control*, *30 October–2 November 2012, Singapore, Singapore,* B. Indraratna, et al., Eds. Research Publishing, 2012, pp. 209–222, doi: 10.3850/978-981-07-3559-3_103-0002.

[14] S. Kwiecień and J. Sękowski, *Stone columns formed with the use of dynamic replacement technology*. Gliwice, Poland: SUT Press, 2012 (in Polish).

[15] J. Sękowski, S. Kwiecień, and P. Kanty, " Field tests of rammed stone columns shape with the use of electrical resistivity tomography", *Inżynieria Morska i Geotechnika*, no. 4, pp. 523–527, 2013 (in Polish).

[16] A. Danilewicz, "Numerical simulation of column creating process by dynamic replacement method", PhD thesis, Gdańsk University of Technology, Gdańsk, 2014 (in Polish).

[17] S. Kwiecień and M. Kowalska, "Dynamic Replacement: the influence of pounder diameter and ground conditions on shape and diameter of the columns", *Architecture Civil Engineering Environment*, vol. 16, no. 1, pp. 71–84, 2023, doi: 10.2478/acee-2023-0005.

[18] PN-EN ISO 17892-12:2018-08 Geotechnical investigation and testing. Laboratory testing of soil. Part 12: Determination of liquid and plastic limits. PKN, 2018.

[19] R. Jasiński, K. Stebel, and J. Domin, "Application of the DIC technique to remote control of the hydraulic load system", *Remote Sensing*, vol. 12, no. 21, art. no. 3667, 2020, doi: 10.3390/rs12213667.

Badania laboratoryjne wpływu wybranych parametrów technologicznych na proces formowania kolumn metodą wymiany dynamicznej

Słowa kluczowe: grunt słaby, kolumny kamienne, wymiana dynamiczna, wzmacnianie podłoża gruntowego

Streszczenie:

Wymiana dynamiczna jest jedną z metod wzmacniania podłoża w ramach inżynierii geotechnicznej, w trakcie której formowane są w podłożu kolumny z gruntu gruboziarnistego o frakcji od piaszczystej do kamienistej. Technologia formowania kolumn wydaje się prosta: kolejne zrzuty ubijaka o masach od 5 do 20 ton, z wysokości 15–25 m, wprowadzają wbijany materiał w podłoże, a powstały krater jest sukcesywnie zasypywany. Wtłaczany materiał przemieszcza się pionowo, ale i również poziomo w podłoże wzmacniane, a jednym z parametrów decydujących o kształcie uzyskiwanych kolumn jest stosunek miąższości wzmacnianego podłoża (H_s) do wysokości ubijaka (H_p). Z doświadczeń krajowych autorów wynika jednak, że w praktyce często dochodzi do wykonania kolumn zawieszonych w warstwach słabych o miąższości powyżej 4,5 m ($H_s/H_p \geq 2,25$), pomimo tego, że na świecie znane są realizacje w warstwach o miąższościach większych (nawet do 8–9 m). Powodem wykonania kolumn zawieszonych może być przyjęcie błędnej technologii formowania kolumn, na którą składają się: energia uderzenia ubijaka (E_t), głębokość wykonania krateru (H_{cr}), wysokość (objętość) jego zasypu (V_{cr}) oraz przyjęte uziarnienie materiału kolumn (d_m). Skłoniło to autorów artykułu do podjęcia badań o wspomnianym zakresie – w pierwszym etapie w warunkach laboratoryjnych. Badania były prowadzone na stanowisku w postaci prostopadłościennej skrzyni o zewnętrznych wymiarach 1,5 m (szerokość) × 1,0 m (wysokość) × 0,15 m (grubość), wyposażonej od czoła w akrylową szybę, umożliwiającą obserwację procesu wbijania materiału w słabą warstwę w skali technicznej 1:10. Warstwę słabą modelował usieciowany polimer akrylowy zmieszany z wodą w stosunku 1:15 (wagowo) o miąższości 2,5 krotnie większej od wysokości stosowanego ubijaka ($H_s/H_p = 2,5$), warstwę nośną z kolei piasek średni o uziarnieniu 0,063–2 mm, a kolumny wykonywano ze: żwiru MGr_1 o uziarnieniu 2–16 mm ($d_m/D_{bp} = 0,022–0,18$), żwiru MGr_2 o uziarnieniu 2–32 mm ($d_m/D_{bp} = 0,022–0,36$) oraz piasku średniego MSa o uziarnieniu 0,063–2 mm ($d_m/D_{bp} \leq 0,022$), gdzie $D_{bp} = 90$ mm to średnica podstawy ubijaka. Proces formowania kolumn był rejestrowany aparatem cyfrowym i kamerą o częstotliwości nagrywania 100 kl/s, a następnie analizowany w programie GOM i Autocad. Przewidziano wykonanie trzech typów kolumn, różniących się głębokością krateru początkowego: (A) $H_{cr} = 0.2$ m ($H_{cr}/H_s = 0,4$), (B) $H_{cr} = 0,3$ m ($H_{cr}/H_s = 0,6$) and (C) $H_{cr} = 0,4$ m ($H_{cr}/H_s = 0,8$). Krater był zasypywany materiałem w 50% (kolumny A_50), 75% (kolumny B_75, C_75) albo w 100% (kolumny A_100, B_100, C_100). Dla wytypowania optymalnej głębokości krateru (H_{cr}) oraz wielkości jego zasypu (V_{cr}) zastosowano materiał MGr_1, a następnie sprawdzono wpływ zastosowania dwóch

pozostałych materiałów o innym uziarnieniu (MGr_2 i MSa). Przeprowadzone badania unaoczniły znaczny wpływ badanych parametrów technologicznych na proces formowania kolumn oraz ich końcowy kształt. Konieczna do zastosowania energia uderzenia rośnie wraz z głębokością początkowego krateru oraz z objętością jego zasypu. Trzon formowanych kolumn, dla których krater początkowy spełniał warunek $H_{cr}/H_s = 0, 6$–$0,8$ ulegał w trakcie wbijania obrotowi, co dało ostatecznie kolumny zawieszone bądź tylko punktowo oparte na warstwie nośnej, o nieregularnych kształtach. W przypadku krateru o najmniejszej głębokości ($H_{cr}/H_s = 0, 4$), w pełni zasypywanego ($V_{cr} = 100\%$), od początku formowana była podstawa w kształcie półkolistym, powiększająca się i pogrążająca się w trakcie wykonywania kolumny. W efekcie, uzyskano kolumny o kształcie „gruszki", oparte punktowo na warstwie nośnej. Kolumny oparte całkowicie na warstwie nośnej i o średnicy zwiększającej się wraz z głębokością udało się ukształtować w przypadku kraterów o najmniejszej głębokości, zasypywanych w połowie ($V_{cr} = 50\%$) (typ A_50). Jak wynika z badań polowych i analiz numerycznych MES, przeprowadzonych wcześniej przez jednego z autorów, tego typu kolumny charakteryzują się największą nośnością i sztywnością. Dodatkowo, do ich wykonania wymagana była mniejsza energia uderzenia, w porównaniu z kolumnami typu B i C. Najlepsze wyniki uzyskano dla kolumn formowanych z materiału o uziarnieniu $d_m/D_{bp} = 0, 022$–$0,18$. W przypadku materiału drobniejszego ($d_m/D_{bp} \leq 0, 022$) ubijak penetrował zasyp krateru, zmniejszając efektywność formowania kolumn o odpowiedniej długości oraz nadmiernie powiększając średnice głowic. Z kolei materiał o większym uziarnieniu ($d_m/D_{bp} = 0, 022$–$0,36$) klinował się w skrzyni badawczej, uniemożliwiając wykonanie powtarzalnych kolumn w warunkach laboratoryjnych. Powyższe badania pozwoliły na sformułowanie wstępnych wytycznych formowania kolumn, spełniających warunek $H_s/H_p = 2, 5$, $H_{cr} = H_p$. Mianowicie: $V_{cr} = 50\%$ przy zrzutach 1–22 i $V_{cr} = 100\%$ przy zrzutach 23–28. Pierwsze 11 zrzutów formuje trzon kolumny – w ich trakcie stosunek wpędu podstawy kolumny (S_c) do wpędu ubijaka (S_p) wynosi kolejno: 0,28–0,2–0,15–0,11–0,06–0,05–0,04–0,04–0,04–0,03–0,02. Kolejne 11 zrzutów formuje podstawę, a ostatnie 11 zrzutów wykonywanych jest przy pełnym zasypie krateru ($V_{cr} = 100\%$). Wytyczne te wymagają weryfikacji w warunkach polowych.